Effects of the Sintering Temperature on RF Complex Permeability of NiCuCoZn Ferrites for Near-Field Communication Applications

Poonam Lathiya and Jing Wang

University of South Florida, Tampa, FL 33620 USA

The effect of bismuth oxide (Bi_2O_3) and sintering temperature on NiCuCoZn ferrite powders has been investigated for the near-field communication applications. The powders were prepared by conventional solid-state synthesis method. The microstructure and frequency-dependent complex permeability were investigated. Employment of Bi_2O_3 as a sintering aid promotes uniform grain growth and densification in sintered powders, which in turn has affected complex permeability spectra. It has been observed that the addition of Bi_2O_3 decreases permeability and magnetic loss from 147 to 110 and from 0.03 to 0.02, respectively, which were both sintered at 1100 °C and measured at 13.56 MHz frequency as compared to undoped sample (without Bi_2O_3). Also, permeability and magnetic loss were increased with sintering temperature. Complex permeability and resonance frequency follow the Globus model.

Index Terms— **Complex permeability, magnetic loss tangent, near-field communication (NFC), Ni–Cu–Co–Zn ferrites.**

I. Introduction

RECENTLY, radio frequency identification technology is a newly emerging field for wireless communications. In particular, near-field communication (NFC) operating at 13.56 MHz is very attractive for many application areas such as wireless power transfer, mobile transactions, identity tags, and access control [1]. In NFC systems, a magnetic ferrite thin sheet is inserted between antennas and metal case to reduce eddy currents generated on the metallic surface and to enhance the power transfer efficiency. To elevate the performance, a thin magnetic sheet of a high permeability and low magnetic loss is required [2], [3]. Soft magnetic ferrites are viewed as the most promising materials because of their high permeability, low losses, high resistivity, and high Curie temperature for employment of low- and high-frequency applications near the NFC frequency of 13.56 MHz. Ni–Zn ferrites hold desirable properties among all ferrites due to their high resistivity, high permeability, and low losses at HF, very high frequency, or even UHF frequencies [2]. These properties of Ni–Zn ferrites depend on the chemical composition, microstructure, choice of additives, and preparation method that can be modified easily through different synthesis parameters such as sintering temperature, reactant ratio, and added dopants [4]–[7]. Enhancement of the magnetic property and Q-factor with varied strategic choice of dopants in Ni–Zn ferrites has been reported [8], [9]. Addition of dopants such as Co_2O_3, V_2O_5, CaO, and Bi_2O_3 as a sintering aid helps to lower the sintering temperature, thus resulting in low magnetic loss and better permeability [10]–[12]. Complex permeability and magnetic loss depend on domain-wall motion and spin domain rotation. Domain-wall motion, in turn, is influenced by grain growth [13]. High sintering temperature leads to abrupt grain growth, which induces higher magnetic loss in ferrites. In this paper, we demonstrated the effect of sintering temperature on the complex permeability of Ni–Cu–Co–Zn ferrites at RF frequencies with and without addition of Bi_2O_3 as the sintering aid. The complex permeability and resonance frequency of Ni–Cu–Co–Zn ferrites have followed the predictions of the Globus model [14].

Manuscript received June 5, 2018; revised July 24, 2018; accepted September 8, 2018. Date of publication October 3, 2018; date of current version January 18, 2019. Corresponding author: P. Lathiya (e-mail: poonam2@mail.usf.edu).

Digital Object Identifier 10.1109/TMAG.2018.2870885

II. Experimental Setup

A. Synthesis of Ferrites

$Ni_{0.33}Cu_{0.2}Co_{0.014}Zn_{0.456}Fe_{1.96}O_{3.94}$ ferrites were prepared via solid-state reaction synthesis [9]. All the constituent raw materials, Fe_2O_3, ZnO, CuO, NiO, and Co_2O_3 were weighed according to their respective molecular weight percentages and wet mixed together in a planetary ball mill for 2 h. After drying the powder, calcination was done at 800 °C for 2 h. The calcined powders were then divided into two portions and one portion is dry ball milled with 0.2 wt% Bi_2O_3 for 2 h at the speed of 560 rpm. Then, both portions of fine powders (with and without Bi_2O_3) were mixed with 10 wt% polyvinyl alcohol binder to make toroidal samples with an outer diameter of 7 mm, an inner diameter of 3.1 mm, and a height of 3 mm. Finally, the doped and undoped samples were sintered in air at 1100 °C and 1120 °C for 2 h.

B. Characterization of Ferrites

Calcined powders were analyzed by X-ray diffraction using Cu-K_α radiation to study the phase composition. The microstructure of the sintered samples was observed by scanning electron microscopy (Hitachi S800 SEM, Krefeld, Germany). Complex permeability of ferrite samples was measured by an impedance analyzer (E4991A, 1 MHz–1 GHz analyzer, Keysight) and a magnetic material test fixture (Keysight 16454A).

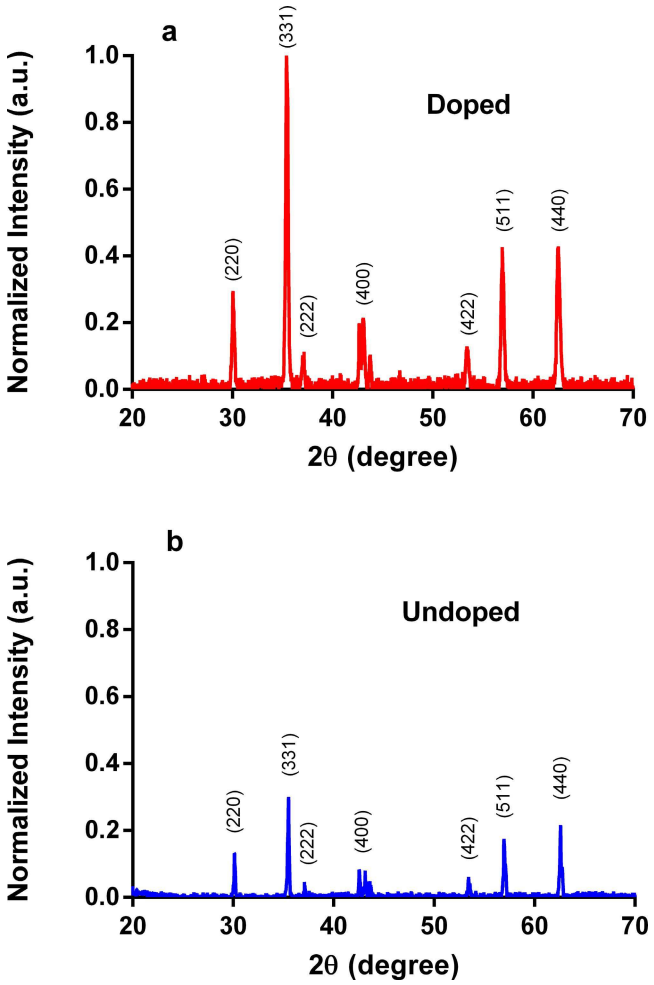

Fig. 1. X-ray diffraction patterns of $Ni_{0.33}Cu_{0.2}Co_{0.014}Zn_{0.456}Fe_{1.96}O_{3.94}$ powders sintered at (a) 1100 °C for doped (0.2 wt% Bi_2O_3, red curve) and (b) undoped (no Bi_2O_3, blue curve) samples.

III. Results and Discussion

Fig. 1 shows the XRD patterns of both doped and undoped $Ni_{0.33}Cu_{0.2}Co_{0.014}Zn_{0.456}Fe_{1.96}O_{3.94}$ specimens sintered at 1100 °C. A single-phase cubic spinel structure is observed in both the samples, with no secondary phase peak. There is no bismuth peak observed in the doped sample as the percentage of Bi_2O_3 (0.2 wt%) is too small to be observed. Nevertheless, the intensity of the doped sample is stronger as compared to the undoped sample as shown in Fig. 1. The addition of Bi_2O_3 intensify the spinel phase formation in the reaction, hence, the grains were arranged in more crystalline form [12].

The surface morphology of $Ni_{0.33}Cu_{0.2}Co_{0.014}Zn_{0.456}Fe_{1.96}O_{3.94}$ ferrite samples was characterized using SEM. Fig. 2 shows the SEM images of ferrite samples with and without bismuth dopants sintered at two different temperatures of 1100 °C and 1120 °C. All SEM images were taken from the surface of the sintered toroid specimens. The grain growth and densification of sintered samples are highly dependent on the presence of Bi_2O_3 in the samples [12]. It can be seen from Fig. 2(a) and (b) that the addition of 0.2 wt% Bi_2O_3 promotes more uniform grain growth and facilitates densification. As compared to undoped samples (without Bi_2O_3), doped specimens (0.2 wt% Bi_2O_3) exhibited more uniform

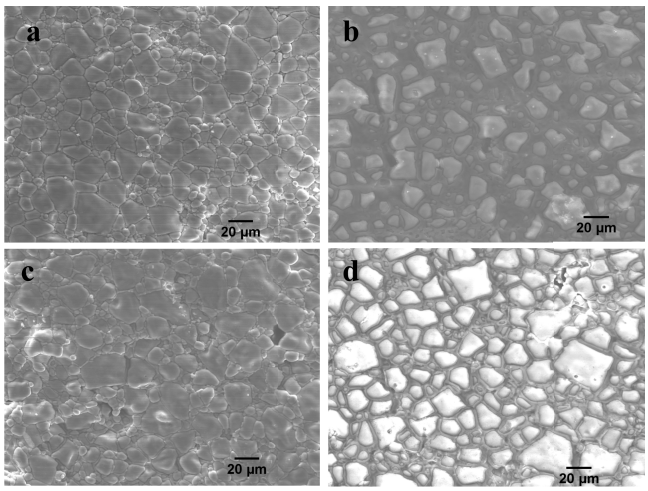

Fig. 2. SEM images of NiCuCoZn ferrite sintered (a) doped and (b) undoped at 1100 °C and (c) doped and (d) undoped at 1120 °C.

grain growth and reduction of pores. At 1100 °C, average grain size for doped (with bismuth oxide) samples lies between 15 and 20 μm, while for the undoped sample, grain size lies between 15 and 25 μm. Bi_2O_3 is a low melting point (820 °C) additive, which forms liquid phase during sintering, as the chosen sintering temperatures of 1100 °C and 1120 °C are much higher than the melting point of Bi_2O_3. Hence, it enhances grain growth that leads to the densification as shown in Fig. 2.

In addition, higher densification and more abnormal grain growth were observed with an increase in the sintering temperature as shown in Fig. 2(c) and (d). At 1120 °C, average grain size lies between 25 and 30 μm for the doped sample. Similar trend was observed for the undoped sample at 1120 °C with average grain size lies between 20 and 30 μm. It can be confirmed that sintering at higher temperature induces a more abnormal grain growth and an increase of intragranular porosity. In undoped samples, dual microstructures were observed, consisting of both small grains and uncontrolled large grains. This can be ascribed to non-uniform grain growth and partial burnout of the binder.

The dependence of complex permeability on frequency is termed as permeability dispersion. The frequency dependent complex relative permeability is given as [15]

$$\mu_r = \mu' - j\mu'' \tag{1}$$

where μ_r is the ratio of permeability of the material versus that of the free space (μ_0). μ' and μ'' are the real and imaginary parts of the complex permeability, respectively.

The magnetic loss tangent is given as

$$\tan\delta_m = \frac{\mu'}{\mu''}. \tag{2}$$

The measured frequency-dependent complex permeability spectra and magnetic loss tangent of the doped and undoped $Ni_{0.33}Cu_{0.2}Co_{0.014}Zn_{0.456}Fe_{1.96}O_{3.94}$ samples, which are sintered at 1100 °C and 1120 °C, are depicted in Fig. 3. It is noticed that the addition of 0.2 wt% of Bi_2O_3 in the ferrite powders decreases real and imaginary parts of permeability and the magnetic loss tangent as compared to undoped samples

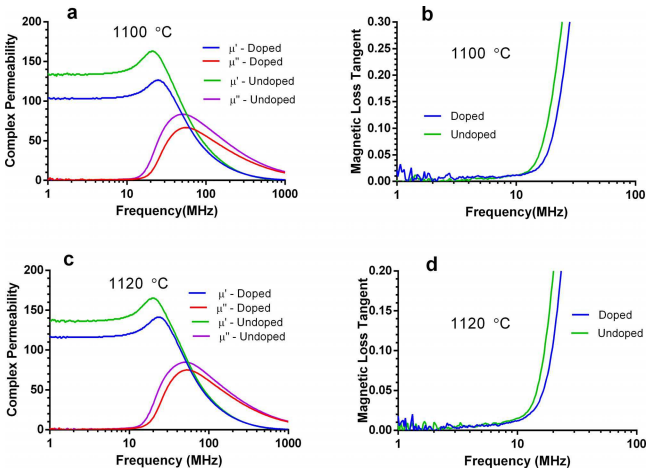

Fig. 3. Complex permeability spectra of NiCuCoZn ferrite sintered at 1100 °C. (a) Complex permeability. (b) Magnetic loss tangent for doped and undoped samples and 1120 °C. (c) Complex permeability. (d) Magnetic loss tangent for doped and undoped samples.

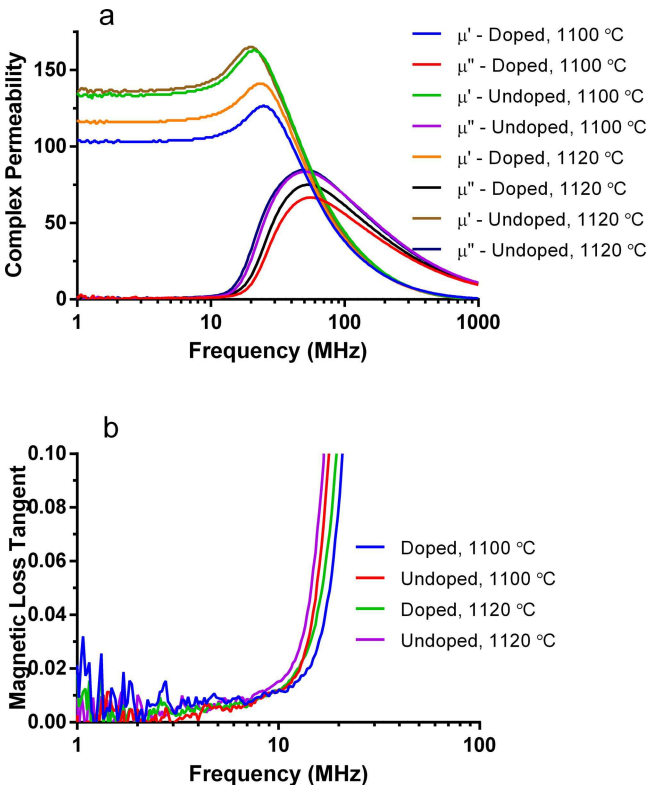

Fig. 4. Comparison of (a) complex permeability spectra and (b) magnetic loss of NiCuCoZn ferrite sintered at 1100 °C and 1120 °C for doped and undoped samples.

as shown in Fig. 3(a) and (b) for 1100 °C. The relative permeability decreases from 147 to 110, while the specimen is doped by 0.2 wt% of bismuth at 1100 °C. Meanwhile, magnetic loss tangent is also lowered from 0.026 to 0.018 due to the addition of bismuth that promoted more uniform grain growth and pore size reduction as compared to undoped samples. Similarly, at 1120 °C, as grain growth of particles is more, an increase in real and imaginary parts of permeability; hence, increase in magnetic loss was observed for both doped and undoped samples sintered at 1120 °C as observed in Fig. 3(c) and (d) due to abnormal grain growth.

TABLE I
REAL AND IMAGINARY PARTS OF COMPLEX PERMEABILITY, MAGNETIC LOSS TANGENT, Q-FACTOR, AND RESONANCE FREQUENCY OF FERRITE SAMPLES AT 13.56 MHz

Sample	Real Permeability	Imaginary permeability	Magnetic loss	Q-factor	Resonance frequency (MHz)
NiCuCoZn-0.2 wt% Bi_2O_3, 1100 °C	110	1.98	0.018	55.5	24.8
NiCuCoZn-0 wt% Bi_2O_3, 1100 °C	147	3.94	0.026	37.3	21.6
NiCuCoZn-0.2 wt% Bi_2O_3,1120 °C	125	3.1	0.024	40.3	24.8
NiCuCoZn-0 wt% Bi_2O_3,1120 °C	152	5.47	0.035	28	20.6

The comparison between the complex permeability spectra and magnetic loss at both temperatures for the doped and undoped samples are shown in Fig. 4(a) and (b).

According to the Globus model, the product of the resonance frequency and complex permeability of ferrites can be approximately estimated by the following equation [14]:

$$(\mu_i - 1)^2 f_r \approx \text{constant} \tag{3}$$

where μ_i, and f_r are the complex permeability and resonance frequency, respectively. The real and imaginary parts of the complex permeability, magnetic loss tangent, Q-factor, and resonance frequency at 13.56 MHz for doped and undoped samples are listed in Table I.

It can be concluded from the results shown in Table I that the resonance frequency is higher for low-permeability samples. It is anticipated that the low-permeability specimens exhibit demagnetizing fields due to magnetic wall movements that raise the restoring force, thus resulting in an increased resonance frequency [14]. A similar trend is observed in all specimens.

IV. CONCLUSION

The effects of the higher sintering temperature and the addition of bismuth oxide on NiCuCoZn ferrite powders were studied. Bismuth oxide is used as a sintering aid in previous studies to lower the sintering temperature. This paper herein is focused on the effects of higher sintering temperature on the frequency-dependent complex permeability and magnetic loss with and without the usage of a sintering aid. At the elevated temperatures of 1100 °C and 1120 °C with the use of sintering aid, a high value of permeability (110 and 125) and low magnetic loss (0.018 and 0.024) were achieved, respectively. Meanwhile, the undoped sample exhibited a permeability of 142 and 152 along with a magnetic loss tangent of 0.026 and 0.035, respectively. A 31% decrease in magnetic loss has been achieved with a 0.2 wt% Bi_2O_3 dopant in ferrite powders, while a 22.5% drop in real part of permeability (also known as relative permeability) has been obtained. High value of

permeability and low magnetic loss is highly desired to realize high efficiency in NFC applications. NiCuCoZn ferrites offer high permeability and low magnetic loss even after sintering at high temperatures. By controlling the grain growth while burning out the binder properly, high permeability and low magnetic loss can be more readily achieved.

REFERENCES

[1] M. Gebhart, R. Neubauer, M. Stark, and D. Warnez, "Design of 13.56 MHz smartcard stickers with ferrite for payment and authentication," in *Proc. 3rd Int. Workshop Near Field Commun. (NFC)*, Feb. 2011, pp. 59–64.

[2] W. Lee *et al.*, "A simple wireless power charging antenna system: Evaluation of ferrite sheet," *IEEE Trans. Magn.*, vol. 53, no. 7, Jul. 2017, Art. no. 2800605.

[3] C. Stergiou, E. Eleftheriou, and V. Zaspalis, "Enhancement of the near-field UHF RFID with ferrite substrates," *IEEE Trans. Magn.*, vol. 48, no. 4, pp. 1497–1500, Apr. 2012.

[4] N.-N. Jiang, Y. Yang, Y.-X. Zhang, J.-P. Zhou, P. Liu, and C.-Y. Deng, "Influence of zinc concentration on structure, complex permittivity and permeability of Ni–Zn ferrites at high frequency," *J. Magn. Magn. Mater.*, vol. 401, pp. 370–377, Mar. 2016.

[5] H. Su, X. Tang, H. Zhang, L. Jia, and Z. Zhong, "Influences of Bi_2O_3 additive on the microstructure, permeability, and power loss characteristics of Ni–Zn ferrites," *J. Magn. Magn. Mater.*, vol. 321, no. 19, pp. 3183–3186, 2009.

[6] B. Yang and Z. Wang, "The structure and magnetic properties of NiCuZn ferrites sintered via a two-step sintering process," *J. Sol-Gel Sci. Technol.*, vol. 80, no. 3, pp. 840–847, 2016.

[7] Z. Zheng, Q. Feng, Q. Xiang, Z. Di, and V. G. Harris, "Low-loss NiZnCo ferrite processed at low sintering temperature with matching permeability and permittivity for miniaturization of VHF-UHF antennas," *J. Appl. Phys.*, vol. 121, no. 6, p. 063901, 2017.

[8] H. Su, H. Zhang, X. Tang, B. Liu, and Y. Jin, "High Q-factor NiCuZn ferrite with nanocrystalline ferrite particles and Co_2O_3 additives," *Phys. Status Solidi A*, vol. 204, no. 2, pp. 576–580, 2007.

[9] X. Wu, S. Yan, W. Liu, Z. Feng, Y. Chen, and V. G. Harris, "Influence of particle size on the magnetic spectrum of NiCuZn ferrites for electromagnetic shielding applications," *J. Magn. Magn. Mater.*, vol. 401, pp. 1093–1096, Mar. 2016.

[10] K. Kawano, M. Hachiya, Y. Iijima, N. Sato, and Y. Mizuno, "The grain size effect on the magnetic properties in NiZn ferrite and the quality factor of the inductor," *J. Magn. Magn. Mater.*, vol. 321, no. 16, pp. 2488–2493, 2009.

[11] B. P. Rao, C.-O. Kim, and C. G. Kim, "Influence of V_2O_5 additions on the permeability and power loss characteristics of Ni–Zn ferrites," *Mater. Lett.*, vol. 61, no. 7, pp. 1601–1604, 2007.

[12] K. Sun, Z. Lan, Z. Yu, L. Li, J. Huang, and X. Zhao, "Grain growth, densification and magnetic properties of NiZn ferrites with Bi_2O_3 additive," *J. Phys. D, Appl. Phys.*, vol. 41, no. 23, p. 235002, 2008.

[13] T. Tsutaoka, "Frequency dispersion of complex permeability in Mn–Zn and Ni–Zn spinel ferrites and their composite materials," *J. Appl. Phys.*, vol. 93, no. 5, pp. 2789–2796, 2003.

[14] S. Kumar, T. Shinde, and P. Vasambekar, "Engineering high permeability: Mn–Zn and Ni–Zn ferrites," *Int. J. Appl. Ceram. Technol.*, vol. 12, no. 4, pp. 851–859, 2015.

[15] P. Parsons, K. Duncan, S. P. Karna, and J. Q. Xiao, "Tailored electromagnetic properties of NiZn nanocomposite materials," in *Proc. IEEE 14th Int. Conf. Nanotechnol. (IEEE-NANO)*, Aug. 2014, pp. 87–91.